NASA Technical Paper 1612

Friction and Wear of Iron-Base Binary Alloys in Sliding Contact With Silicon Carbide in Vacuum

Kazuhisa Miyoshi and Donald H. Buckley

MAY 1980

NASA

NASA Technical Paper 1612

Friction and Wear of Iron-Base Binary Alloys in Sliding Contact With Silicon Carbide in Vacuum

Kazuhisa Miyoshi and Donald H. Buckley
Lewis Research Center
Cleveland, Ohio

Summary

An investigation was conducted to determine the effect of alloying elements (Ti, Cr, Mn, Ni, Rh, and W) on the friction and alloy transfer behaviors of various iron-base, binary, solid-solution alloys in sliding contact with a single-crystal silicon carbide {0001} surface in the ⟨10$\overline{1}$0⟩ directions in vacuum. All multipass sliding-friction experiments were conducted with a load of 0.2 newton, at a sliding velocity of 3×10^{-3} meter per minute for a total sliding distance of 2.5 millimeters, in a vacuum of 10^{-8} pascal at room temperature.

The results of the investigation indicate that the atomic size and concentration of alloy elements play important roles in controlling alloy transfer and the friction properties of iron-base binary alloys. Alloys of high solute concentration produce more transfer than do alloys of low solute concentration. The coefficient of friction generally increases with an increase in the concentration of alloying element. The change of friction with succeeding passes after the initial pass increases as the solute-to-iron atomic-radius ratio increases or decreases from unity.

Introduction

The atomic size and concentration of alloying element are extremely important, not only from a point of view of abrasive wear and friction behavior of alloys, but also of adhesive wear and friction (refs. 1 and 2).

In the abrasion of alloys (in oil, which minimizes adhesion effects on friction and wear) the friction and wear generally decrease with increasing solute concentration. The correlation of solute-to-iron atomic-radius ratio with friction and wear appears to be very good. Friction and wear decrease as the solute-to-iron atomic-radius ratio increases or decreases from unity (ref. 1).

In contrast, the adhesion and static friction of alloys in contact with a single-crystal silicon carbide {0001} surface (in vacuum, which adhesion effects on friction) generally increase with an increase in solute concentration. They also increase as the solute-to-iron atomic-radius ratio of alloys increases or decreases from unity (ref. 2).

This investigation was conducted to determine the effects of alloying elements (such as Ti, Cr, Mn, Ni, Rh, and W) on the friction, adhesive wear, and transfer of an iron-base, binary-solid-solution-alloy pin in sliding contact with a single-crystal silicon carbide {0001} flat in the ⟨10$\overline{1}$0⟩ direction. Experiments were conducted with a load of 0.2 newton, at a sliding velocity of 3×10^{-3} meter per minute with a total sliding distance of 2.5 millimeters in a vacuum of 10^{-8} pascal, at room temperature. The alloys were all polycrystalline.

Materials

Table I presents the analyzed compositions in atomic percent, of the iron-base alloys used in the present investigation. The iron-base binary alloys were prepared by Stephens and Witzke (ref. 3) who arc-melted the high-purity iron and high-purity alloying elements (Ti, Cr, Mn, Ni, Rh, and W). The solute concentrations ranged from approximately 0.5 atomic percent for those elements that have extremely limited solubility in iron up to approximately 16 atomic percent for these elements that form a series of solid solutions with iron.

The single-crystal silicon carbide was a 99.99-percent-pure compound of silicon and carbon and had a hexagonal-close-packed crystal structure. The composition, structure, and microhardness data, of the single-crystal silicon carbide flats are also shown in table II.

Experimental Apparatus and Procedure

Apparatus

The apparatus used in the investigation measures adhesion, load, and friction. It was mounted in an ultrahigh vacuum system, which also contained tools for surface analysis, an Auger emission spectrometer (AES), and a low-energy-electron diffraction (LEED) system. The mechanism used for measuring adhesion, load, and friction is shown schematically in figure 1. A gimbal-mounted beam is projected into the vacuum system. The beam contains two flats machined normal to each other with two strain gages mounted thereon. The 0.79-millimeter-radius alloy pin is mounted on the end of the beam. As a load is applied by moving the beam in the direction normal to the disk, it is measured by the strain gage. The vertical sliding motion of the pin along the flat surface is

TABLE I.—CHEMICAL ANALYSIS AND SOLUTE-TO-IRON ATOMIC RADIUS RATIOS FOR IRON-BASE BINARY ALLOYS

Solute element	Analyzed solute content, at.% (a)	Analyzed interstitial content, ppm by weight (a)			Solute-to-iron atomic radius ratios (b)
		C	O	P	
Ti	1.02	56	92	7	1.1476
	2.08	--	---	--	↓
	3.86	87	94	9	
	8.12	--	---	--	
Cr	0.99	--	---	--	1.0063
	1.98	50	30	12	↓
	3.92	--	---	--	
	7.77	40	85	10	
	16.2	--	---	--	
Mn	0.49	--	---	--	0.9434
	.96	39	65	6	↓
	1.96	--	---	--	
	3.93	32	134	8	
	7.59	--	---	--	
Ni	0.51	--	---	--	0.9780
	1.03	28	90	6	↓
	2.10	--	---	--	
	4.02	48	24	5	
	8.02	--	---	--	
	15.7	38	49	7	
Rh	1.31	--	---	--	1.0557
	2.01	20	175	22	↓
	4.18	--	---	--	
	8.06	12	133	19	
W	0.83	30	140	12	1.1052
	1.32	--	---	--	↓
	3.46	23	61	21	
	6.66	--	---	--	

[a]Ref.3.
[b]Refs, 3, 10, and 11.

TABLE II. - SINGLE-CRYSTAL SILICON CARBIDE MATERIAL DATA

(a) Composition[a]

Si	C	O	B	P	Others
66.6%	33.3%	<500 ppm	<100 ppm	<200 ppm	<0.1 ppm

(b) Crystal structure

Interatomic distance, Å		Lattice ratio, c/a
a	c	
3.0817	15.1183	4.9058
3.073	15.070	4.9069

(c) Hardness data

Plane	Direction	Knoop hardness number (b)
(0001)	$\langle 11\bar{2}0 \rangle$	2670
(0001)	$\langle 10\bar{1}0 \rangle$	2825

[a]Manufacturer's analyses.
[b]Load, 2.9 N.

Figure 1. - High-vacuum friction and wear apparatus.

CD-11718-15

accomplished through a motorized gimbal assembly. Under an applied load the friction force is measured during vertical translation of the strain gage mounted normal to that used to measure load. This feature was used to examine the coefficient of friction at various loads, as shown in figure 1.

Specimen Preparation

The iron-base binary alloy pins and silicon carbide flats were polished with 3-micrometer-diameter diamond powder and then a 1-micrometer-diameter aluminum oxide (Al_2O_3) powder. Both the pin and flat surfaces were rinsed with 200-proof ethyl alcohol.

The specimens were placed in the vacuum chamber, which was evacuated and baked out to a pressure of 1.33×10^{-8} pascal (10^{-10} torr), whereupon argon gas was bled back into the vacuum chamber to a pressure of 1.3 pascals. A 1000-volt, direct-current potential was applied, and the specimens (both flat and pin) were argon sputter bombarded for 30 minutes. After the sputtering operation was completed, the vacuum chamber was reevacuated, and AES (Auger emission spectroscopy) spectra of the flat surface were obtained to determine the degree of surface cleanliness. When the desired

degree of cleanliness of the flat was achieved, friction experiments were conducted.

Experimental Procedure

A load of 0.2 newton was applied to the pin-flat contact by defecting the beam (fig. 1). Both load and friction force were continuously monitored during a friction experiment. Sliding velocity was 3×10^{-3} meter per minute for a sliding distance of 2.5 millimeter per pass and a total sliding distance of 25 millimeters in 10 passes. All friction experiments were conducted with the system evacuated to 10^{-8} pascal.

Results and Discussions
Cleanliness of Silicon Carbide Surface

An Auger emission spectrum of the single-crystal silicon carbide {0001} surface was obtained before sputter cleaning. The crystal was in the as-received state before it had been baked out in the vacuum system. In addition to the silicon and carbon peaks, an oxygen peak is evident. The oxygen peak and chemically shifted silicon peaks at 78 and 89 electron volts (eV) indicate a layer of SiO_2 on the silicon carbide surfaces as well as a simple, adsorbed film of oxygen (refs. 4 to 6). The Auger spectrum taken after the silicon carbide surface had been sputter cleaned clearly revealed silicon and carbon peaks at 92 and 272 eV, respectively; the oxygen peak was negligible.

Tribological Behavior

Friction.—Multipass sliding-friction experiments were conducted with iron-base binary alloys of various solute concentrations in contact with single-crystal silicon carbide in vacuum. The binary-alloy systems were iron alloyed with titanium, chromium, manganese, nickel, rhodium, or tungsten. Figure 2 shows a typical friction-force trace resulting from such multipass sliding. The trace is characterized by a sharp break in the friction force at points b, that is, stick-slip behavior. The a-b regions represent the process where the loading and tangential (shear) forces are being applied to the specimen, but where no gross sliding occurs. Point b is the onset of slip. In the b-c region, the surfaces of the alloy and silicon carbide are in rapid slip. Point c may be located at the same place as point a, and after the first cycle they are the same.

The coefficient of friction μ is defined as $\mu = \bar{F}_{max}/W$, where $\bar{F}_{max}$ is the average friction force
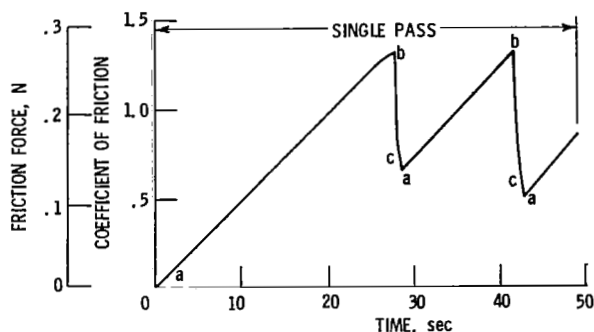

Figure 2. – Typical friction force trace for 8.12 at. % Ti-Fe alloy sliding on single-crystal silicon carbide 0001 surface. Load, 0.2 N.
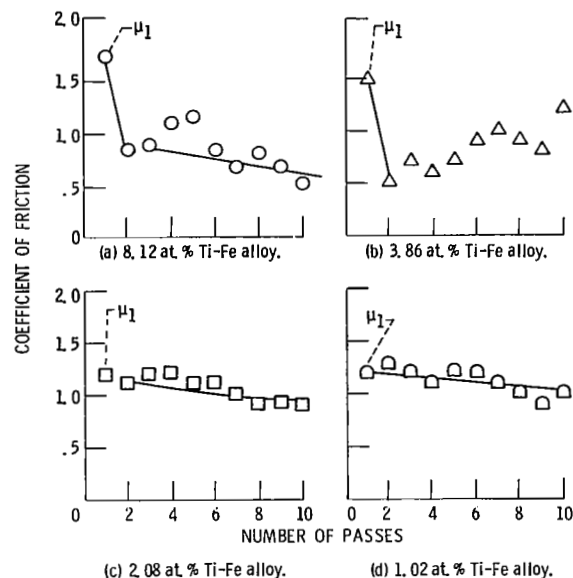

Figure 3. – Average coefficient of friction calculated from maximum peak heights in friction trace, as function of number of passes of Ti-Fe alloy pins across single-crystal silicon carbide {0001} surface. Load, 0.2N.

calculated from maximum peak heights (b in fig. 2) in which the sharp breaks are observed in the friction force trace and W is the normal load.

Figures 3 and 4 present typical data of the coefficients of friction as a function of the number of passes. When repeated passes are made, the coefficients of friction for alloys having a high solute concentration or chemically active alloying elements (Mn, Ni, Ti) generally decrease with number of passes (see figs. 3(a) and (b)). The coefficients of friction for first-pass sliding differ a great deal from those for the second and subsequent passes. This is due to the large amount of alloy transfer to the
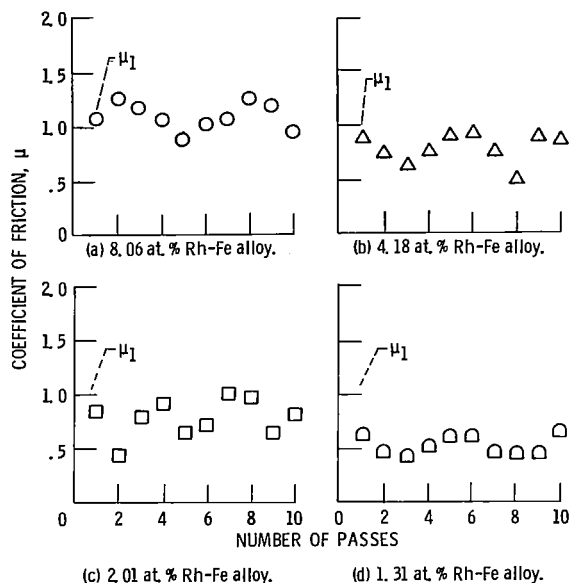
(a) 8.06 at.% Rh-Fe alloy. (b) 4.18 at.% Rh-Fe alloy.

(c) 2.01 at.% Rh-Fe alloy. (d) 1.31 at.% Rh-Fe alloy.

Figure 4. - Average coefficient of friction, calculated from maximum peak heights in friction trace, as function of number of passes of Rh-Fe alloy pins across single-crystal silicon carbide {0001} surface. Load, 0.2 N.
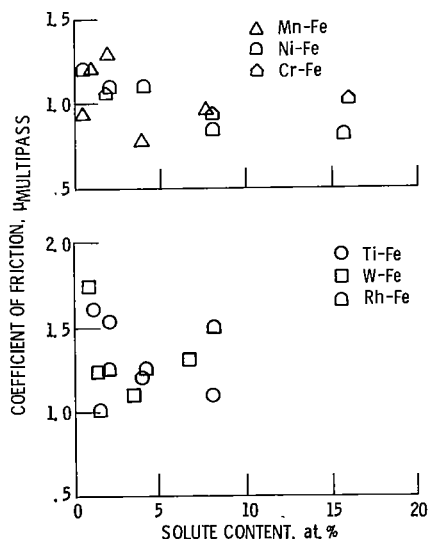

(a) 8.12 at.% Ti-Fe alloy transfer.

(b) 2.68 at.% Ti-Fe alloy transfer.

Figure 6. - Wear tracks on SiC flat revealing transfer of Ti-Fe pin alloys to flat. Scanning electron micrographs; SiC {0001} surface; number of passes, 10; load, 0.2 N.

Figure 5. - Coefficient of friction for various iron-base binary alloys as function of solute content. Multipass sliding on single-crystal silicon carbide {0001} surface; sliding direction, $\langle 10\bar{1}0 \rangle$; sliding velocity, 3 mm/min; load, 0.2 N; room temperature; vacuum pressure, 10^{-8} Pa.

silicon carbide surface in the first pass of the rider (ref. 2). The alloy transfer and its influence on friction will be discussed in succeeding sections. Once the transfer starts in the first pass, the phenomenon of multipass slidings is that the alloy is in essence sliding against itself. This influences subsequent friction properties, alloy transfer to the silicon carbide, and the nature of the transfer film. This finding is consistent with earlier studies, by Peterson and Lee (ref. 7) and by the present authors (ref. 8), of metals sliding against nonmetals and manganese-zinc ferrite.

On the other hand, the coefficients of friction for the alloy having low solute concentration or chemically less active alloying elements (Rh) generally exhibit small but fluctuating changes with the

(a) 4.18 at.% Rh-Fe alloy transfer.

(b) 1.31 at.% Rh-Fe alloy transfer.

Figure 7. - Wear tracks on SiC flat revealing transference of Rh-Fe pin alloys to flat. Scanning electron micrographs; SiC {0001} surface; number of passes, 10; load, 0.2 N.

solute of rhodium and chromium, the coefficients of friction during multipass sliding changed only slightly with increasing solute concentration.

Transfer of alloys.—Inspection of the single-crystal silicon carbide flat surfaces after sliding contact with the alloys revealed the presence of metallic elements, indicating transfer of the alloy to silicon carbide. This transfer occurred even with a single-pass sliding of the alloy pin on silicon carbide (ref. 2). Figures 6 and 7 show scanning electron micrographs of wear tracks on the silicon carbide surfaces generated by 10 passes of iron-base binary alloys. It is obvious that the copious amounts of alloy transfer to the silicon carbide occur with multicontact sliding. As may be seen in figures 6 and 7, alloys having high solute content (table I) produce more transfer than do alloys having low solute content. In general, the wear produced by the multipass sliding of these
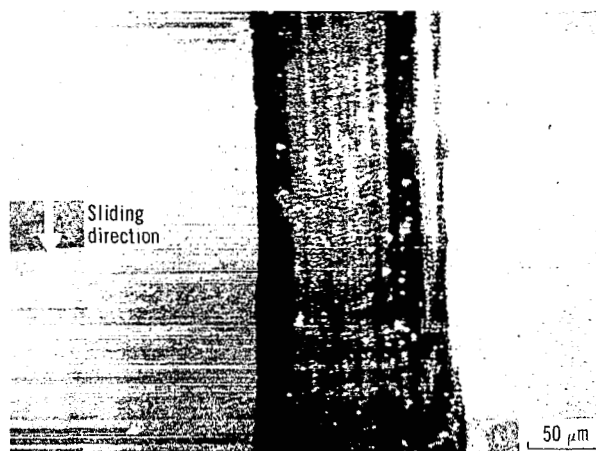

Figure 8. - Wear track on SiC flat showing wear debris and transfer film of 1.02 at.% Ti-Fe pin. Scanning electron micrographs; SiC {0001} surface; number of passes, 10; load, 0.2 N.

number of passes (as typified in figures 3(c) and (d) and 4). The fluctuating behavior of the coefficient of friction also strongly depends on the nature of the transfer of the alloys. Again, the transfer of alloy to the silicon carbide influences subsequent friction properties and the wear of alloys, which are dependent on the material properties. For the iron-base binary alloys with titanium, tungsten, nickel, and manganese, the coefficients of friction during multipass sliding generally decrease as the solute concentration increases (fig. 5). The trend is completely opposite that of the static-friction behavior discussed in reference 2; in that work, the static friction of alloys in contact with silicon carbide was found to increase with an increase in solute concentration without exception. For iron-base binary alloys with

Figure 10. - Fracture of SiC flat as a result of sliding contact with 4.18 at % Rh-Fe pin. Scanning electron micrograph; SiC {0001} surface; load, 0.2 N.
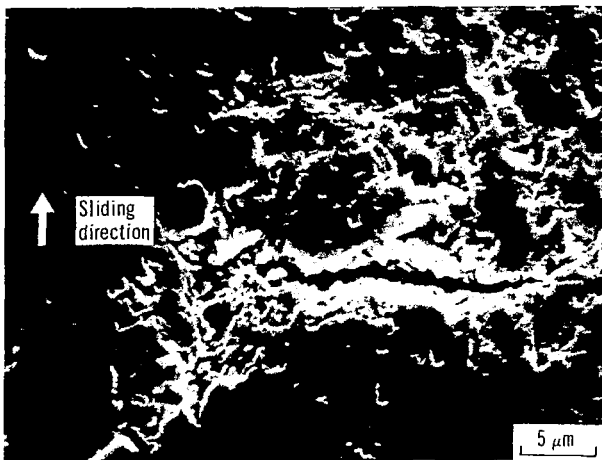

Figure 9. - Wear scar on 8.12 at.% Ti-Fe pin showing grooves, indentations, and fractures. Scanning electron micrographs; SiC {0001} surface; number of passes, 10; load 0.2 N.

alloys on silicon carbide can be categorized in this way: (1) a very thin transfer film on the contact area, (2) multilayer transfer films, (3) very small particles (submicron), and (4) piled-up particles (several micrometers). The small particles are seen in or near the wear track (fig. 8(a)); the piled-up larger particles are seen beside the weak track (fig. 8(b)).

Wear.—The wear scars on all the alloy riders showed evidence of a large number of plastically deformed grooves, indentations, and cracks (fig. 9). The grooves and indentations were the result of plowing by transferred alloy debris on silicon carbide and/or the sliding and rolling of wear debris of silicon carbide and alloy. The cracks propagate perpendicular to the sliding direction in the wear scar of the alloy. The cracks initiate and propagate, with maximum shear stresses in the weakest interfacial
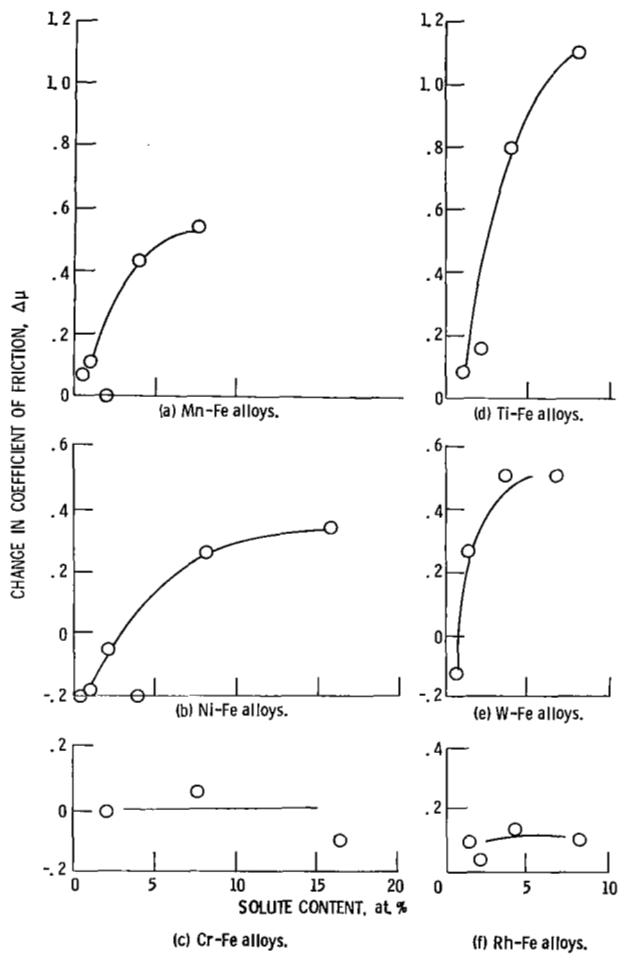
region of the alloy where both loading and tangential forces are being applied to the interface.

The wear tracks on the silicon carbide surfaces showed evidence of (1) alloy transfer to silicon carbide (as already mentioned) and (2) fracture pits and cracks in the silicon carbide surfaces. The scanning electron micrograph of figure 10 indicates that an exceptionally large fracture crack results in the silicon carbide from the repeated loading and unloading during multipass slidings. The fracture is due to cleavages of the {0001}, {10$\bar{1}$0}, and {11$\bar{2}$0} planes. Even with single-pass sliding, however, cracks were observed (ref. 2). This is consistent with earlier studies (refs. 2, 4, and 9) and is discussed in more detail in reference 9.

Influence of Alloy Transfer on Friction

Figures 11 and 12 present the change and the rate of change of the coefficient of friction with the number of passes as a function of solute concentrations (atomic percent) at a load of 0.2 newton. The changes were estimated from the data, as typically shown in figures 3 and 4. The changing of the coefficient of friction is expressed as $\mu_1 - \mu_{multipass} = \Delta\mu$ in figure 11, and $\Delta\mu/\mu_1$ in figure 12, where μ_1 is the coefficient of friction for first pass sliding and $\mu_{multipass}$ is the average coefficient of friction calculated from the coefficients of friction for second- to tenth-pass slidings. The change of coefficient of friction generally increases as the solute concentration increases, with the exceptions of rhodium and chromium, and the increasing rate of change of coefficient of friction strongly depends on the alloying element.
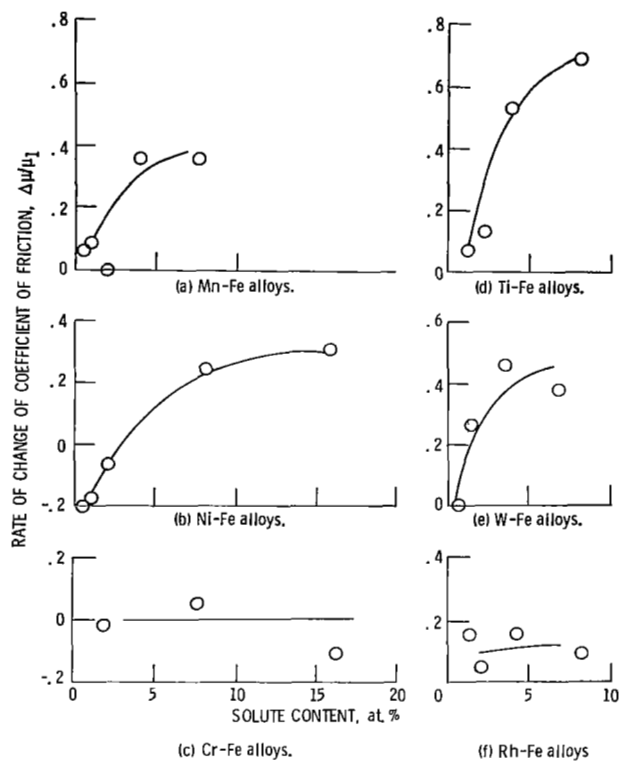
Figure 11. – Changing of coefficient of friction with number of passes as function of solute content.

Figure 12. – Rate of change of coefficient of friction with number of passes as function of solute content.
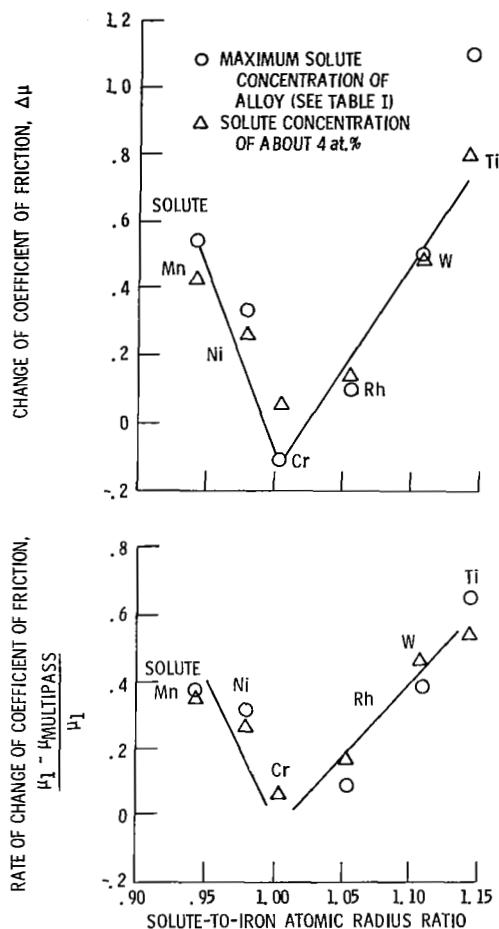
Conclusions

The following conclusions are drawn from the data presented herein:

1. The atomic size and concentration of the alloying element are factors in controlling friction during multipass slidings; that is, the coefficient of friction generally increases with an increase in the concentration of alloying element. The change of coefficient of friction with succeeding passes increases after the initial pass as the solute-to-iron atomic radius ratio increases or decreases from unity.

2. Alloys having high solute concentration produce more transfer than do alloys having low solute concentrations.

3. All of the alloys examined transferred to the surfaces of silicon carbide on sliding.

Lewis Research Center,
National Aeronautics and Space Administration,
Cleveland, Ohio, November 16, 1979,
506–16.

References

1. Miyoshi, Kazuhisa; and Buckley, Donald H.: Friction and Wear With a Single-Crystal Abrasive Grit of Silicon Carbide in Contact With Iron-Base Binary Alloys in Oil—Effects of Alloying Elements and Content. NASA TP – 1394, 1979.

2. Miyoshi, Kazuhisa; and Buckley, Donald H.: Adhesion and Friction of Iron-Base Binary Alloys in Contact with Silicon Carbide in Vacuum. NASA TP – 1604, 1980.

3. Stephens, Joseph R.; and Witzke, Walter R.: Alloy Softening in Binary Iron Solid Solutions. J. Less-Common Metals, vol. 48, Aug. 1976, pp. 285 – 308.

4. Miyoshi, Kazuhisa; and Buckley, Donald H.: Friction and Metal Transfer for Single-Crystal Silicon Carbide in Contact With Various Metals in Vacuum. NASA TP – 1191, 1978.

5. Johannesson, J.S.; Spicer, W.E.; and Strausser, Y.E.: An Auger Analysis of the SiO_2-Si Interface. J. Appl. Phys., vol. 47, no. 7, July 1976, pp. 3028 – 3037.

6. Miyoshi, Kazuhisa; and Buckley, Donald H.: Effect of Oxygen and Nitrogen Interactions on Friction of Single-Crystal Silicon Carbide. NASA TP – 1265, 1978.

7. Peterson, M.B.; and Lee, R.E. Jr.: Sliding Characteristics of the Metal-Ceramic Couple. Wear, vol. 7, 1964, pp. 334 – 343.

8. Miyoshi, Kazuhisa; and Buckley, Donald H.: Frictrion and Wear of Single-Crystal and Polycrystalline Manganese-Zinc Ferrite in Contact With Various Metals. NASA TP – 1059, 1977.

9. Miyoshi, Kazuhisa; and Buckley, Donald H.: Wear Particles of Single-Crystal Silicon Carbide in Vacuum. NASA TP – 1624, 1980.

10. Hume-Rothery, W.; and Ragnor, G.V.: The Structure of Metals and Alloys. Fourth ed. rev., The Institute of Metals (London), 1962, pp. 246 – 258.

11. Wyman, L.L.; and Park, J.J.: Table of Periodic Properties of the Elements. Naional Bureau of Standards, USCOMM – DC – 28,801, 1961.

Figure 13. – Change of coefficient of friction as function of solute-to-iron atomic-radius ratio.

Therefore, those changes were plotted as a function of material, that is, the solute-to-iron atomic-radius ratio, in figure 13. There appears to be very good correlation between the rates of change of the coefficient of friction with number of passes and the solute-to-iron atomic-radius ratio. That correlation is separated into two cases: first, for alloying with manganese and nickel, which have smaller atomic radii than iron; and second, for chromium, rhodium, tungsten, and titanium, which have larger atomic radii than iron. The changes $\Delta\mu$ or $\Delta\mu/\mu_1$ increase as the solute-to-iron atomic-radius ratio increases or decreases linearly from unity. Thus, the correlations indicate that the atomic size of the solute is an important parameter in the change of the coefficient of friction during multipass sliding.